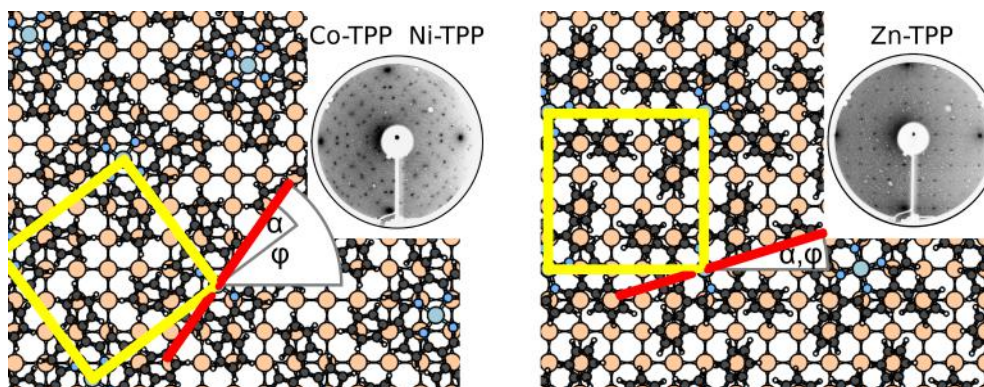=0pt
Graphical Abstract

Elusive central-atom dependence in the adsorption of M-TPP molecules (M=Co, Ni, Zn) on Fe(001)-
$p(1 \times 1)$**O**

Guido Fratesi,Simona Achilli,Aldo Ugolotti,Alessandro Lodesani,Andrea Picone,Alberto Brambilla,Luca Floreano,Alberto Calloni,Gianlorenzo Bussetti

Highlights

Elusive central-atom dependence in the adsorption of M-TPP molecules (M=Co, Ni, Zn) on Fe(001)-$p(1 \times 1)$O

Guido Fratesi,Simona Achilli,Aldo Ugolotti,Alessandro Lodesani,Andrea Picone,Alberto Brambilla,Luca Floreano,Alberto Calloni,Gianlorenzo Bussetti

- Theoretical and experimental analysis of Co-, Ni-, and Zn-TPP on Fe(001)-$p(1 \times 1)$O

- Calculations foresee very small differences between the Co-, Ni-, and Zn-TPP films

- Similarities in the adsorption configurations and energetics confirm tunability

- Small differences trigger perceivable changes in the overlayer alignment

Elusive central-atom dependence in the adsorption of M-TPP molecules (M=Co, Ni, Zn) on Fe(001)-$p(1 \times 1)$O

Guido Fratesi[a,b,*], Simona Achilli[a], Aldo Ugolotti[c], Alessandro Lodesani[d], Andrea Picone[d], Alberto Brambilla[d], Luca Floreano[e], Alberto Calloni[d] and Gianlorenzo Bussetti[d]

[a]*Dipartimento di Fisica "Aldo Pontremoli", Università degli Studi di Milano, I-20133 Milano, Italy*

[b]*European Theoretical Spectroscopy Facility (ETSF)*

[c]*Dipartimento di Scienza dei Materiali, Università degli Studi di Milano-Bicocca, I-20125 Milano, Italy*

[d]*Dipartimento di Fisica, Politecnico di Milano, p.za Leonardo da Vinci 32, I-20133 Milano, Italy*

[e]*Istituto Officina dei Materiali – CNR-IOM, Laboratorio TASC s.s 14 km 163.5, 34149 Trieste, Italy*

ARTICLE INFO

ABSTRACT

Metal-tetraphenyl-porphyrin (M-TPP) molecules typically self-assemble forming square-like super-lattices, as dictated by the shape of the molecule. The dependence of the adsorption properties on the central atom is systematically studied for Co-, Ni-, and Zn-TPP adsorbed on oxygen passivated Fe(001), namely the Fe(001)-$p(1 \times 1)$O surface. It is found by low energy electron diffraction (LEED) and scanning tunneling microscopy (STM) that despite the weak molecule-substrate interaction, preserving many features of quasi-free molecules, the self-assembled structure switches from the $(5 \times 5)R37°$ superlattice of Co-TPP and Ni-TPP to the plain (5×5) of Zn-TPP. Ab initio calculations based on density functional theory (DFT) are used to investigate the adsorption properties of the different molecules and the possible overlayers formed. Adsorption energies and structures and electronic properties are reported, discussing the bonding mechanisms and the magnetic character. Only moderate energy differences are found, suggesting that subtle effects may steer the selection of the structure among overlayers with similar properties although differing substantially as for the LEED and STM experimental results.

1. Introduction

Modern technology considers thin and ultra-thin films composed by organic molecules key steps for the development of new generation devices: advanced electronics, sensors, optical instruments, bio-compatible systems, etc. [1, 2] Organic molecules synthesis allows to obtain compounds with specific and tunable electronic and mechanical properties, which represents an important characteristic when junctions and interfaces must be realized. [3] For a long time now, among the different organic compounds, porphyrins and porphyrinoid molecules have shown special properties that make this class of organic molecules almost unique and exploitable for applications. [4] In particular, the basic porphyrin system is composed by an almost flat tetra-pyrrolic macrocycle. At the skeleton border, four phenyl groups are linked to the main cavity of the molecule. A metal ion (e.g., Co, Ni, Zn, etc.) can be placed inside the central ring, and its presence can alter the characteristic optical and electronic properties of the molecule. This represents the structure of the so-called metal tetra-phenyl porphyrin (M-TPP). It is noticeable that different transition metal ions can be placed inside the porphyrin cavity without changing the physical structure of the molecule. This occurrence appears as a natu-

ral way of tuning the chemical, electronic and transport properties of the molecule

A 2-D scalable device requires an ordered assembly of molecules onto a substrate. [4] In this respect, M-TPPs usually show a square-lattice super-structure when the very first layer is grown onto several substrates with different surface crystal orientations, [4] such as silver, [5, 6] gold, [7, 8] copper, [9, 10, 11] metal-oxides, [12, 13, 14] graphite, [15] etc. These observations suggest that the porphyrin square skeleton drives the molecular assembling. Being linked by a single C-C bond to the main porphyrin ring, the phenyl groups can be reoriented in view of minimizing the molecule-molecule interaction in the deposited film. [16] From these data, it is reasonable to consider M-TPP a prototype system where the different regions of the molecule (inner cavity and border skeleton/phenyl groups, respectively) exhibit different chemical and physical properties. This assumption represents a practical guide in many experiments when a specific organic/inorganic interface must be grown. Unfortunately, a direct check of this hypothesis and possible limitations have been never investigated in details yet.

In this work we study the structural and electronic properties of highly ordered Co-, Ni- and Zn-TPP single layers, realized by exploiting a particular substrate, namely oxygen-passivated Fe(001) or Fe(001)-$p(1 \times 1)$O, formed by adsorbing a single layer of O atoms on the four-fold hollow sites of the Fe surface lattice. [17, 18] As extensively investigated in our previous studies involving various molecules [12, 19] and also other metallic surfaces [20], the ultra-thin oxide layers resulting from surface passivation are able to efficiently

*Corresponding author

✉ guido.fratesi@unimi.it (G. Fratesi)

ORCID(s): 0000-0003-1077-7596 (G. Fratesi); 0000-0001-6812-5043 (S. Achilli); 0000-0002-4894-070X (A. Ugolotti); 0000-0002-2834-6893 (A. Lodesani); 0000-0001-7920-6893 (A. Picone); 0000-0002-5593-317X (A. Brambilla); 0000-0002-3654-3408 (L. Floreano); 0000-0002-7389-2703 (A. Calloni); 0000-0001-8556-8014 (G. Bussetti)

decouple the deposited molecules, which retain their compositional integrity and a minimally perturbed electronic structure with respect to the freestanding case. In addition, Fe and other 3rd row transition metals are able to induce a magnetic order in the adsorbed porphyrin molecules, a characteristic of interest for spintronic applications [21, 22].

The structure and morphology of the porphyrin layers is investigated by low-energy electron diffraction (LEED), scanning tunneling microscopy (STM) and near edge X-ray adsorption fine structure spectroscopy (NEXAFS), juxtaposed to a detailed theoretical study that tries to find a rationale to similarities and differences between the studied M-TPP films. According to the M-TPP tunability hypothesis, calculations foresee very small differences between the Co-, Ni- and Zn-TPP films. Conversely, experimental data show a significant change in, e.g., the assembling properties of the molecules. This suggests that small changes in the used molecules can trigger perceivable difference in the realized interfaces.

2. Materials and Methods

2.1. Experimental methods

The Fe(001)-$p(1 \times 1)$O substrate was prepared in a ultra high vacuum (UHV) system (base pressure of 10^{-8} Pa) by exposing the clean Fe(001) surface to 30 L (1L = 1.33 × 10^{-4} Pa s) of molecular oxygen at 450 °C and annealing at about 700 °C.[23]. Porphyrins were sublimated in a dedicated chamber by means of Knudsen effusion cells held at a temperature of about 300 °C. The deposition flux, measured by means of a quartz microbalance, was 0.5 ML/min , being 1 ML= 3.06 Å. [24]

The STM measurements were performed by using an Omicron variable temperature STM in a UHV chamber connected to the preparation system. STM images were acquired at room temperature in constant-current mode with home-made electrochemically etched W tips. Near edge X-ray adsorption spectroscopy (NEXAFS) data were acquired at the Elettra synchrotron (ALOISA beamline) in partial electron yield mode. Spectra were collected with the light impinging on the sample surface at a grazing angle (6°) and the electric field either parallel (*s*-polarization) or perpendicular (*p*-polarization) to the surface. The photon flux normalization and the energy calibration were performed as described in Ref. [25]. The photon energy resolution was set to 80 × 10^{-3} eV. All experiments were performed at room temperature under negligible charging conditions.

2.2. Theoretical methods

We have analyzed the system by ab initio calculations within density functional theory (DFT), taking the vdW-DF-c09 functional [26] that includes dispersion forces for exchange and correlation. Calculation with periodically repeated cells, ultrasoft pseudopotentials, and plane waves, have been executed by the Quantum ESPRESSO simulation package. [27, 28] For pseudopotentials, we have followed our previous work for Co-TPP on the same substrate [29] and used files generated from scalar-relativistic all-electron calculations, as avail-

able from the Quantum-ESPRESSO website (those adopted in our previous studies for Fe and O [30] and for Co, [31, 32]) from pslibrary [33] for Ni, H, C and N, and from the Quantum ESPRESSO website for Zn. The cutoff for plane wave expansion was set to 36 Ry and to 220 Ry for the wavefunctions and electron density, respectively.

We model the Fe(001)-$p(1 \times 1)$O surface by a four-layer Fe slab, where the bottom two are fixed at the bulk interlayer distance, and O is adsorbed on the top side as in our previous works. [30] We sample the Brillouin zone of the supercell adopted in the calculation by a 2×2 shifted Monkhorst-Pack grid, [34] that would corresponds to a 10×10 sampling in the conventional Brillouin zone of Fe(001). Geometry optimization of molecular coordinates is then performed until the forces on atoms are lower than 0.1 mRy/Bohr. For Co-TPP, we include the DFT+U correction to improve the treatment of on-site correlation at the metal atom. We consider the rotationally-invariant form with a single parameter $U_{\text{eff}} = U - J = 3.0$ eV, resulting from $U = 4.0$ eV and $J = 1.0$ eV as proposed in several works [35, 36, 37, 38]. While the absence of the +U correction provides a too low-energy Co state in the unoccupied spin-minority manifold, coordinates and energies with/without the +U correction are very similar as we show next.

3. Results and Discussion

3.1. Diffraction and microscopy

Figure 1 displays LEED measurements acquired after deposition of 1 ML of Co-TPP, Ni-TPP and Zn-TPP on the Fe(001)-$p(1 \times 1)$O substrate, along with the sketch showing the reciprocal lattices of the corresponding molecular overlayers. The sharp diffraction patterns observed for each M-TPP indicate the presence of highly ordered self assembled monolayers. In each LEED image are visible also four intense spots corresponding to the reciprocal lattice of the substrate, which allows to establish the epitaxial relation between the Fe(001)-$p(1 \times 1)$O surface lattice vectors $\mathbf{a}_i$ and those of the overlayers $\mathbf{a}'_i$: $\mathbf{a}'_i = M_{ij}\mathbf{a}_j$, with M being the epitaxy matrix. The Co-TPP [29] and Ni-TPP overlayers form a $(5 \times 5)R37°$ superlattice with respect to the substrate where rotational domains having $M_{ij} = \left(\begin{smallmatrix} 4 & 3 \\ -3 & 4 \end{smallmatrix}\right)$ or $M_{ij} = \left(\begin{smallmatrix} 3 & 4 \\ -4 & 3 \end{smallmatrix}\right)$, respectively, give rise to the sets of spots indicated in the bottom panel of Figure 1. Conversely, Zn-TPP arrange in a (5×5) superstructure [16] with the same matrix $M_{ij} = \left(\begin{smallmatrix} 5 & 0 \\ 0 & 5 \end{smallmatrix}\right)$ regardless of the rotational domains observed by STM.

Figure 2 reports STM constant current images at a large scale (top row) and at a smaller one where individual molecules are identifiable (bottom row). STM images confirm that M-TPP molecules form compact and ordered wetting layers, as testified also by the fast Fourier transform that we report for each top panel as its inset. It is interesting to notice that in the case of Ni-TPP the boundaries between different rotational domains form straight and well defined lines along the main crystallographic direction of the substrate, while in the case of Co-TPP they are more disordered and run along the [110]
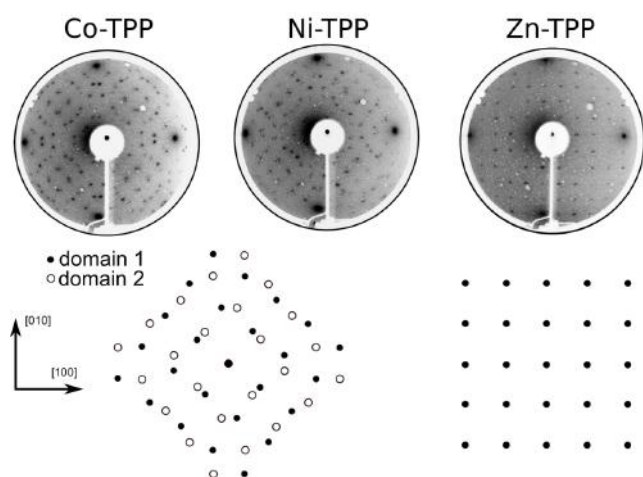
Figure 1: Measured LEED patterns (beam energy 55 eV) for 1 ML of Co-TPP (left), Ni-TPP (middle) and Zn-TPP (right) deposited on Fe(001)-$p(1 \times 1)$O. The intense spots visible in the screens periphery arise from the Fe(001)-$p(1 \times 1)$O surface. The bottom part reports the schematic LEED patterns corresponding to $(5 \times 5)R37°$ (left) and (5×5) (right) molecular superstructures.
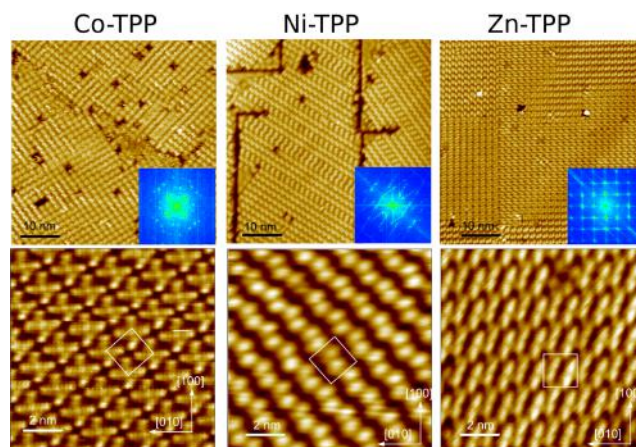
Figure 2: STM images acquired at 50×50 nm^2 (top row) and 10×10 nm^2 (bottom row) for 1 ML of Co-TPP (left, tunneling parameters $V = 1.4$ V and $I = 1$ nA), Ni-TPP (middle, $V = 2$ V and $I = 0.5$ nA) and Zn-TPP (right, $V = 2$ V and $I = 1$ nA) deposited on Fe(001)-$p(1 \times 1)$O. The insets of top panels display the corresponding fast Fourier transforms. The square drawn in each bottom panel marks the unit cell of the molecular overlayer.

axis. The zoomed images of Figure 2 reveal for Ni-TPP and Zn-TPP molecules a twofold symmetry, while Co-TPP are characterized by a fourfold structure. It is important to recall that STM images generally reflect both the topographical and electronic properties of the surface, therefore the images depend on the current flowing across the tunneling junction and on the applied voltage. Besides such a dependence, we also found a strong influence of the tip conformation, therefore it was not possible to establish a straightforward relation between the tunneling parameters and the molecules imaging. Additional information on the geometric structure of each molecule can be inferred by NEXAFS measurements reported hereafter.

3.2. NEXAFS characterization

The NEXAFS results acquired on 1 ML and 4 ML Ni-TPP films are shown in Figure 3 for the N K- and Ni L$_{2,3}$-edges. They complete our previous characterization of the M-TPP system, presented in Ref. [29] and [16] for Co-TPP and Zn-TPP, respectively. The results related to the M-TPP monolayer are compared to those related to a multilayer film, where the molecules are not in direct contact with the Fe(001)-$p(1 \times 1)$O surface.

Thanks to the chemical sensitivity of NEXAFS, our results probe the unoccupied electronic states in the central region of the molecule. N contributes to $2p$ unoccupied states delocalized on the tetrapyrrole ring and characterized by π^* and σ^* symmetry. According to the selection rules for $1s$ to $2p$ electronic transitions, X-ray adsorption is promoted when the light polarization is perpendicular to the nodal plane of such states. In the case of flat-lying aromatic molecules, for instance, π^* symmetry states have their nodal plane coincident with the molecular plane and can be populated with p-polarized light. The N K-edge lineshape and peak posi-

tions closely resemble the results obtained on the Co-TPP system [29, 39]. Features (A-D) observed in p-polarization are related to electronic transitions to π^* orbitals whereas features A' (at 398.7 eV) and E, observed in s-polarization, are related to σ^* resonances. The π^* and σ^* resonances almost vanish in s- and p-polarization, respectively, displaying a large NEXAFS dichroism, which is indicative of a macrocycle closely parallel to the surface and with small off-plane distortion. The same conclusion could be drawn in the Zn-TPP case [16], even if no signal from σ^* symmetry state below the ionization threshold is observed there.

In view of a better comparison with our previous results ([29] and others, reported in the literature [40]), we show the spectra acquired at the Ni L$_{2,3}$-edge, where a strong dichroism is found. In analogy with Ref. [40], we attribute the observed features to σ^* symmetry transitions between Ni $2p$ and $3d_{x^2-y^2}$ states.

3.3. M-TPP adsorption models

We discuss adsorption models for almost-flat-lying M-TPP molecules starting with some general aspects. We take first the simpler case of the (5×5) superstructure (as observed for Zn). In this case, the unit cell of is aligned with [100] and [010] surface azimuths and a ball-stick model is depicted in Figure 4(a) (given the generality of the discussion, and the fact that the various M-TPP coordinates are very similar by visual inspection, in Figure 4 we always report Co-TPP coordinates). With respect to gas phase molecules, phenyl rings in adsorbed porphyrins partially flatten and the pyrrole macrocycle bends in a saddle shape [41], with two opposite pyrrole rings bent inwards and two bent outwards with respect to the surface. Accompanying this distortion, phenyl groups also rotate towards flattening the molecule. The hin-
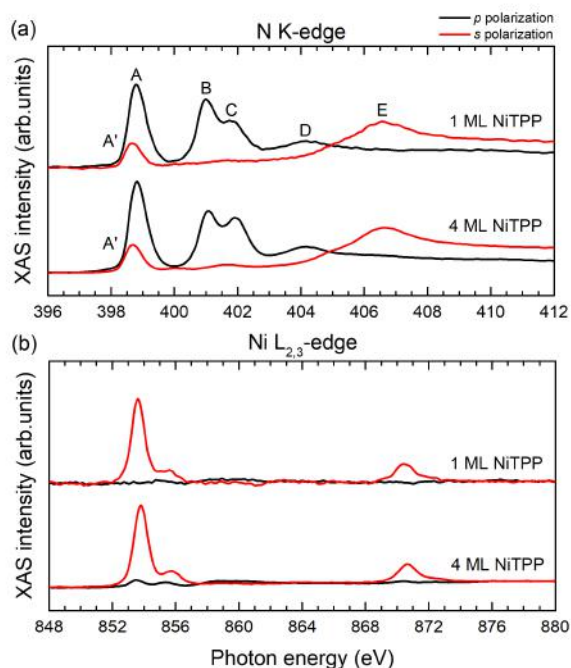
Figure 3: NEXAFS spectra acquired at (a) the N K-edge and (b) the Ni $L_{2,3}$-edge on Ni-TPP/Fe(001)-$p(1\times1)$O for different molecular coverages. Red (black) lines refer to spectra acquired with $s(p)$-polarized light. Letters A-E identify the main spectroscopic features of the spectra in panel (a). Spectra from different coverages have been rescaled for a better comparison.

drance between bulky phenyl terminations of nearby molecules forces the rotation around the normal to the surface, which can be characterized by the angle α formed between the N-M-N direction (joining N atoms of the two inwards-bent pyrroles with the metal ion, indicated in red in the figure panels) and an overlayer lattice vector. In this context, the four phenyl rings are only pairwise equivalent: two marked "a" and "c" face a pyrrole ring from a neighboring molecule bent inwards, whereas the other two, "b" and "d" in the figure, face a pyrrole bent outwards.

A schematic representation of this adsorption mode is provided in Figure 4. For the case of non-rotated (5×5) adsorption, four equivalent domains are found and are depicted in Figure 4(a$^{\mathrm{i}}$-a$^{\mathrm{iv}}$). These domains can be obtained from each other by rotating the molecular overlayer by 90° (a$^{\mathrm{i}}$-a$^{\mathrm{ii}}$, a$^{\mathrm{iii}}$-a$^{\mathrm{iv}}$), or inverting the azimuthal angle sign ($\alpha \to -\alpha$, corresponding to a mirror of the molecules with respect to a plane orthogonal to an overlayer lattice vector) (a$^{\mathrm{i}}$-a$^{\mathrm{iii}}$, a$^{\mathrm{ii}}$-a$^{\mathrm{iv}}$). They all contribute to the same LEED pattern and have been indeed observed by STM for Zn-TPP [16] (see Figure 2). The angle α coincides, in this (5×5) case, with the angle formed between the same N-M-N direction and the Fe [100] azimuth that we denote as ϕ.

To consider $R37°$ overlayers, let us focus on the $\left(\begin{smallmatrix} 4 & 3 \\ -3 & 4 \end{smallmatrix} \right)$ case for which two nonequivalent domains are possible and are depicted in Figure 4(b) and (c). We consider first the case

shown in Figure 4(b), with schematic drawing in panel (b$^{\mathrm{i}}$) therein. A 90° rotation of the molecular overlayer leads to the equivalent structure shown in (b$^{\mathrm{ii}}$). Performing a mirror operation of structures (b$^{\mathrm{i}}$) and (b$^{\mathrm{ii}}$), with respect to a (010) plane, results into the structures (b$^{\mathrm{iii}}$) and (b$^{\mathrm{iv}}$), respectively, both corresponding to a different reconstruction with $M = \left(\begin{smallmatrix} 3 & 4 \\ -4 & 3 \end{smallmatrix} \right)$ and the other set LEED spots.

Remarkably, the case shown in Figure 4(b) is characterized by an equivalent registry of each molecule with the other M-TPPs in the overlayer as well as with the substrate, so the two cases only differ by the relative orientation of the superlattices.

In the $\left(\begin{smallmatrix} 4 & 3 \\ -3 & 4 \end{smallmatrix} \right)$ structures, at variance from the $\left(\begin{smallmatrix} 5 & 0 \\ 0 & 5 \end{smallmatrix} \right)$ structure, switching the azimuthal rotation of the molecules with respect to the overlayer lattice constant (i.e., taking opposite direction for the angle α), leads to two nonequivalent structures, characterized by a different angle formed by the molecules with the [100] azimuth: from $\phi = 37° - \alpha$ as in Figure 4(b) to $\phi = 37° + \alpha$ as in Figure 4(c). Also in the latter case, one has four possible adsorption configurations (c$^{\mathrm{i}}$)-(c$^{\mathrm{iv}}$) again encompassing both the observed reconstructions $\left(\begin{smallmatrix} 4 & 3 \\ -3 & 4 \end{smallmatrix} \right)$ and $\left(\begin{smallmatrix} 3 & 4 \\ -4 & 3 \end{smallmatrix} \right)$. Summarizing, the LEED data cannot distinguish between the two cases of Figure 4(b) and (c) which however differ on an atomistic point of view.

Remarkably, all structures have the same overlayer lattice constant which is an integer multiple of the substrate one, $|\mathbf{a}'| = 5|\mathbf{a}|$ (this is of course made possible as 3,4 are the catheti of a Pythagorean triangle). It is then interesting to compare this findings with other substrates having square symmetry. On Ag(001), both Co-TPP [42] and Zn-TPP [43] adsorb with a rotated cell having epitaxy matrix $M_{ij} = \left(\begin{smallmatrix} 4 & -2 \\ 2 & 4 \end{smallmatrix} \right)$, hence $|\mathbf{a}'| = \sqrt{20}|\mathbf{a}|$ and no equivalent overlayer aligned to surface azimuths can form. Additionally, we mention the case of Co-TPP on Cu(001) exhibiting a $(5 \times 5)R37°$ superstructure for which, however, no plain (5×5) has been reported up to our knowledge [44].

3.4. First-principles investigation

Independently of the above considerations, the adsorption site of the molecules is another degree of freedom. We recall on this respect our previous analysis for Co-TPP on the same surface [29]. There, we investigated the three molecular arrangements discussed above, each with the central metal atom positioned either on top of a surface O or Fe atom. We found that the cases where the N atoms are approximately sitting above O atoms, like all the cases shown in Figure 4, are significantly more stable than those with N above Fe (obtained upon translating the molecules by $a/2$ along both [100] and [010]): the difference of ≈ 0.3 eV is indeed larger than all other differences reported below. For this reason, in this work we study in detail the three adsorption configurations reported in Figure 4 that are named following the position of the metal atom as (5×5)@O (panel a), (5×5)$R37°$@O (panel b), and (5×5)$R37°$@Fe (panel c).

We have performed structural optimizations for Co-TPP, Ni-TPP, and Zn-TPP in the three chosen structures. As said, on the scale of Figure 4 it is hard to distinguish the final
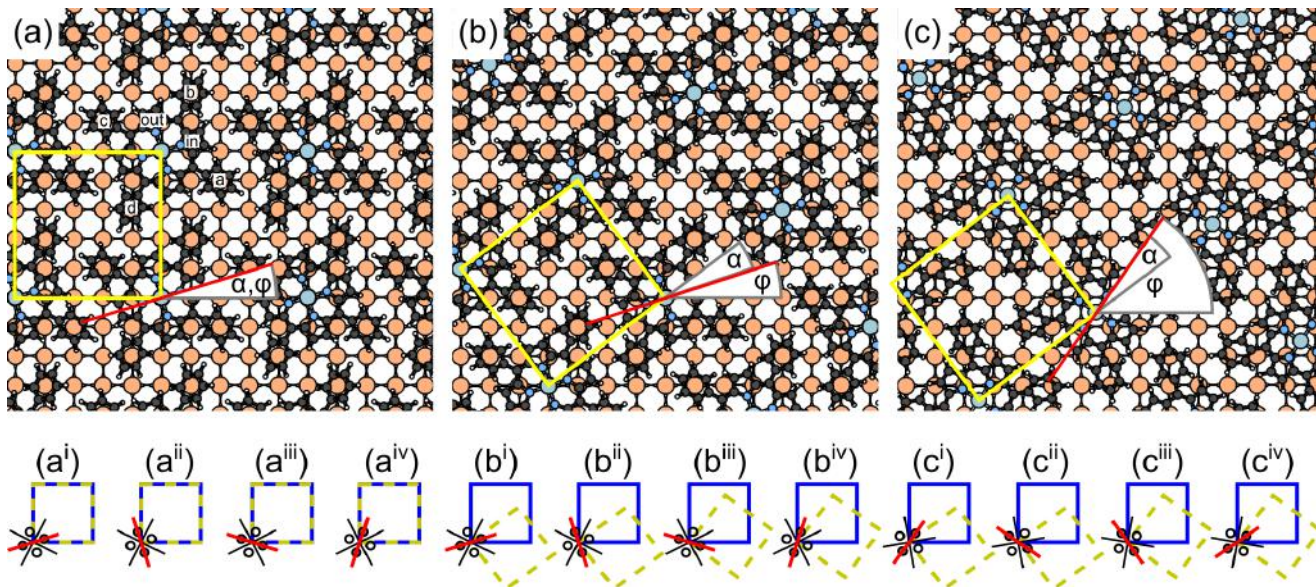
Figure 4: Ball-stick model of three M-TPP adsorption configurations. With (a) (5×5) periodicity at the oxygen site, [named (5×5)@O]; (b) and (c) two configurations with the same $(5 \times 5)R37°$ periodicity, but different molecular azimuth as taken from the [100] axis and adsorption sites [named $(5 \times 5)R37°$@O and $(5 \times 5)R37°$@Fe, respectively]. Yellow squares indicate the surface unit cell; oxygen and iron atoms are identified in orange and white, respectively. Red lines mark the N-M-N direction passing through the pyrrole rings bent inwards; ϕ and α are the angles formed by the red line with the [100] direction and with an overlayer lattice vector, respectively. Labels in panel (a) "in"/"out" are for inwards/outwards bending of pyrrole rings, and "a"-"d" name the phenyl ones. The molecular arrangement in the ball-stick pictures of panels (a-c) is described by the schemes (aⁱ-cⁱ) below. The other schemes (ii-iv) correspond to the energetically equivalent cases that can be obtained through rotations or mirror operations of the overlayer (see the text). The substrate (5×5) cell is depicted as a solid blue square, the overlayer one as a yellow dashed square, and the molecule in black with the red line as above.

structures of the three adsorbates, so we only show there Co-TPP as a representative case. The adsorption energy per molecule is evaluated as $E_{ads} = [E^{tot}_{M\text{-}TPP/surf} - E^{tot}_{M\text{-}TPP} - E^{tot}_{surf}]/N_{M\text{-}TPP}$, where $E^{tot}_{M\text{-}TPP/surf}$ is the total energy of the system with $N_{M\text{-}TPP}$ molecules and $E^{tot}_{M\text{-}TPP}$ and E^{tot}_{surf} those of the optimized free M-TPP and clean surface. We report the results in Table 1. Remarkably, all values lie in an energy range that is only 0.14 eV wide, independently of the central atom and configuration. Also, to evaluate the effect of the on-site correction "+U", we have computed the adsorption energies for Co-TPP switching off the correction and finding practically unchanged values; this suggests that the description of many-body correlation at the metal atom, which may be problematic at the DFT / DFT+U level, is not a crucial issue for determining the adsorption structure. For all molecules, we determine only small differences between the (5×5)@O and the $(5 \times 5)R37°$@O case, or no difference at all for Zn-TPP. We recall from the discussion of Figure 4(a) and (b) that these two configurations in practice present the same intermolecular arrangement and, as seen by a single molecule, a very similar position of the molecule on the substrate so that such similarity could be expected. On the experimental side no indication of a $(5 \times 5)R37°$ periodicity

is found for Zn-TPP, nor of a (5×5) one for Co-TPP. Ni-TPP is the only case where an apparent preference for a rotated vs non-rotated cell is found, with the $(5 \times 5)R37°$@Fe structure being lower in energy by 0.12 eV than the non-rotated one. We attribute this behavior to a site specificity of Ni: by performing additional simulations for the related molecule Ni-porphin on the same surface, we have found a 0.1 eV preference for the Fe site whereas a milder preference for O (< 0.05 eV) is found for Co-porphin and Zn-porphin.

We now analyze the adsorption geometry computed for specific configurations: for Co-TPP and Ni-TPP in the $(5 \times 5)R37°$@Fe, and for Zn-TPP in the (5×5)@O. For Co-TPP, the choice is based on the fact that $(5 \times 5)R37°$@Fe is marginally higher in energy than $(5 \times 5)R37°$@O, but in better agreement with STM observations[29]; as discussed therein, the two configurations are very similar for structural and electronic properties. The azimuthal angle α formed by the molecules with the overlayer lattice vector is practically identical in the three cases and amounts to $\alpha \approx 18°$. The one formed with the [100] surface azimuth, i.e., ϕ, is also very similar or differs by the rotation angle of 37°. The internal degrees of freedom also appear relatively similar. Differences arise because of a shorter (by approximately 0.2 Å)

Table 1
Adsorption energy, E_{ads}, for M-TPP. The last column with ΔE_{ads} takes as a reference the minimum value for that species.

Species	Configuration	E_{ads} (eV)	ΔE_{ads} (eV)
Co-TPP	$(5 \times 5)R37°$@Fe	−4.26	+0.02
	$(5 \times 5)R37°$@O	−4.28	+0.00
	(5×5)@O	−4.26	+0.02
Ni-TPP	$(5 \times 5)R37°$@Fe	−4.34	+0.00
	$(5 \times 5)R37°$@O	−4.24	+0.10
	(5×5)@O	−4.22	+0.12
Zn-TPP	$(5 \times 5)R37°$@Fe	−4.20	+0.07
	$(5 \times 5)R37°$@O	−4.27	+0.00
	(5×5)@O	−4.27	+0.00
Co-TPP	$(5 \times 5)R37°$@Fe	−4.26	+0.03
(computed	$(5 \times 5)R37°$@O	−4.29	+0.00
without $+U$)	(5×5)@O	−4.26	+0.03

molecule-surface distance computed for Zn-TPP, where Zn sits 2.99 Å from the O plane: this is accompanied by a flattening of the pyrroles bent inwards, $\theta_{\text{py}}^{\text{in}} = 10°$ instead of the 15° computed for other molecules. The phenyl rings instead appear to rotate away from the surface plane by a slightly larger angle, 35°–38° for Zn-TPP instead of the 31°–35° of Ni-TPP (and similar for Co-TPP). We remark that these marginal changes lead by themselves to relatively small energy differences; for their description, in Quantum ESPRESSO calculations, we have enforced convergence thresholds for the iterative structural optimization 10 times stricter than the default ones.

Figure 5 reports the simulated STM image computed at negative (panels a-c, −2 V) and positive (a'-c', +2 V) biases. For what concerns the phenyl and pyrrole units, the appearance of the molecule is similar, whereas the luminosity of the central atom is both element and bias dependent. In qualitative agreement to experiments, Co-TPP molecules appear relatively brighter at the center, especially than Zn-TPP for which a dark "cut" joining the pyrrole units bent inwards separates the two halves. We recall, however, that a strong influence of the tip conformation in the experiments prevents to make firm conclusions on this respect.

Additional detail concerning the electronic properties can be evinced by the electronic density of states, projected on the metal (black lines) and molecular (red lines) orbitals. See Figure 6. Consistently with the simulated STM, the orbitals not involving the central atom are only marginally different. They appear, to the resolution of the calculation, weakly influenced by the magnetic character of the underlying substrate: in particular, no specific shift of the spin-majority/spin-minority states (taking the Fe magnetization as reference) is computed, but looking at specific states, a different broadening for the two spin components can be appreciated as a result of larger substrate DOS, such as for the molecular LUMO in the spin-minority population. For what concerns the metal-projected states, similarly to the free molecules, [38] Co-TPP and Ni-TPP have states around the Fermi level whereas all Zn orbitals of Zn-TPP lie far-
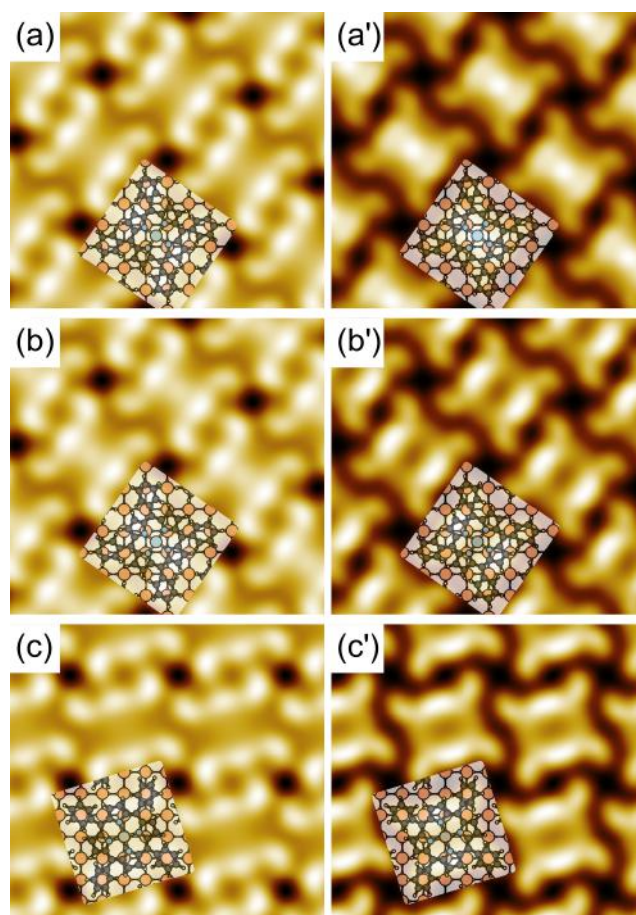
Figure 5: Simulated STM image at −2 V (panel a) and +2 V (panel a') for Co-TPP, and similarly for Ni-TPP, and Zn-TPP in panels (b-b') and (c-c'). A corresponding ball-stick model is overimposed.

ther away. The only case with appreciable spin polarization is Co-TPP, having the spin-down d_{z^2} orbital filled and the spin-up one empty, [29] so that the molecule is antiferromagnetically coupled to the substrate.

The spin polarization of the molecule is better appreciated by looking to the difference between the two spin densities, $\Delta n = n^{\text{up}} - n^{\text{dw}}$, in real space. To this purpose, in Figure 7 we report the difference $\Delta n - \Delta n_{\text{surf}}$, where the spin polarization of the free surface, Δn_{surf}, is characterized by a nearly uniform positive value and is subtracted for a better understanding. In panel (a), the spin polarization of Co-TPP clearly appears with the lobes of a filled d_{z^2} orbital. A much weaker contribution, now parallel to the substrate, is observed around the Ni atom, whereas nothing appears for the chosen isovalue around Zn. Magnetic moments computed by Löwdin analysis [45] for Co, Ni, and Zn amount to −1.09, 0.03, and 0.00 μ_B, respectively. All cases report a small spin-polarization of the macrocycle, parallel to the substrate magnetization, in analogy to what we computed for C_{60} on the same substrate.[46]

We further show real space electron density rearrangements to discuss the bonding mechanisms of the molecules.

Table 2
Structural parameters for adsorption configurations: azimuthal angle ϕ with respect to the [100] direction and α with respect to an overlayer lattice vector (see Figure 4); tilt angles with respect to the surface plane of the pyrrole rings bent inwards/outwards ($\theta_{py}^{in}/\theta_{py}^{out}$) and of phenyl units ($\theta_{ph}$) a, b, c, and d (as labeled in Figure 4, a and c face a pyrrole ring from a neighboring molecule bent inwards whereas b and d face a pyrrole bent outwards); height of the metal atom (z_M) and of N atoms (z_N) taken from the plane of surface O atoms.

Species	Configuration	ϕ (°)	α (°)	θ_{py}^{in} (°)	θ_{py}^{out} (°)	$\theta_{ph}^{a,c}$ (°)	$\theta_{ph}^{b,d}$ (°)	z_M (Å)	z_N^{avg} (Å)
Co-TPP	$(5 \times 5)R37°$@Fe	55	18	15	20	32	35	3.18	3.22
Ni-TPP	$(5 \times 5)R37°$@Fe	55	18	15	21	31	35	3.26	3.29
Zn-TPP	(5×5)@O	17	17	10	21	35	38	2.99	3.09

In Figure 7 we also show the electron density displacement upon adsorption, $n_{M\text{-TPP/subs}} - n_{M\text{-TPP}} - n_{surf}$. By looking to values on a plane passing between the molecules and surface, we can see that an antibonding character at the N atoms is testified by density depletion. Electron density instead accumulates consistently between surface Fe atoms and the outer C atoms of the inward-bent pyrrole units, showing the formation of bonds between Fe and the π orbital; this is best seen for the Zn case in panel (c'); for Co-TPP and Ni-TPP in panels (a') and (b'), instead, such two C atoms are not centered on a Fe atom and one can observe both accumulation (between C-Fe) and depletion (between C-O). Also these results do not show a specific dependence on the central atom (compare Co-TPP and Ni-TPP), beside the different position of the molecule on the surface. We further checked this statement by considering also Zn-TPP in a $(5 \times 5)R37°$ @Fe configuration, which presents the same qualitative findings as for Co-TPP and Ni-TPP (data not shown).

4. Conclusions

Summarizing, we have compared the structural and electronic properties of single-layer Co-TPP, Ni-TPP, and Zn-TPP molecules deposited on Fe(001)-$p(1 \times 1)$O by combining experimental results (LEED, STM, and NEXAFS) and first principles simulations. The molecular overlayers are all characterized by the same square unit cell, whose unit length is five times that of the substrate, consistently with the square shape of the molecules and a moderate molecule-substrate interaction that preserves many features of quasi-free molecules. In all cases, molecules stay nearly parallel to the substrate, with the pyrrole macrocycle bent in a saddle shape and the phenyl rings bent towards the surface. The assembling of the molecules is shown by LEED and STM to switch from the rotated $(5 \times 5)R37°$ superlattice of Co-TPP and Ni-TPP to the (5×5) of Zn-TPP, the latter being aligned with the surface azimuths. This trend may look surprising given both the relatively weak interaction with the substrate, and the same flat lying appearance of the molecules, regardless of the nature of the central atom. Indeed, we find only small differences between the adsorption energy profiles of the three molecular layers, due to the fact that the different molecular arrangements may present very similar char-

acteristics at the atomic scale, in terms of both molecule-surface and molecule-molecule relative positioning. While this hampers finding the rationale beyond the experimentally observed adsorption structure dependence from calculations, it suggests us that assemblying motifs remarkably distinguishable the one from the other on the few-nanometers length scale may actually depend on small and subtle effects at the molecular scale.

Acknowledgments
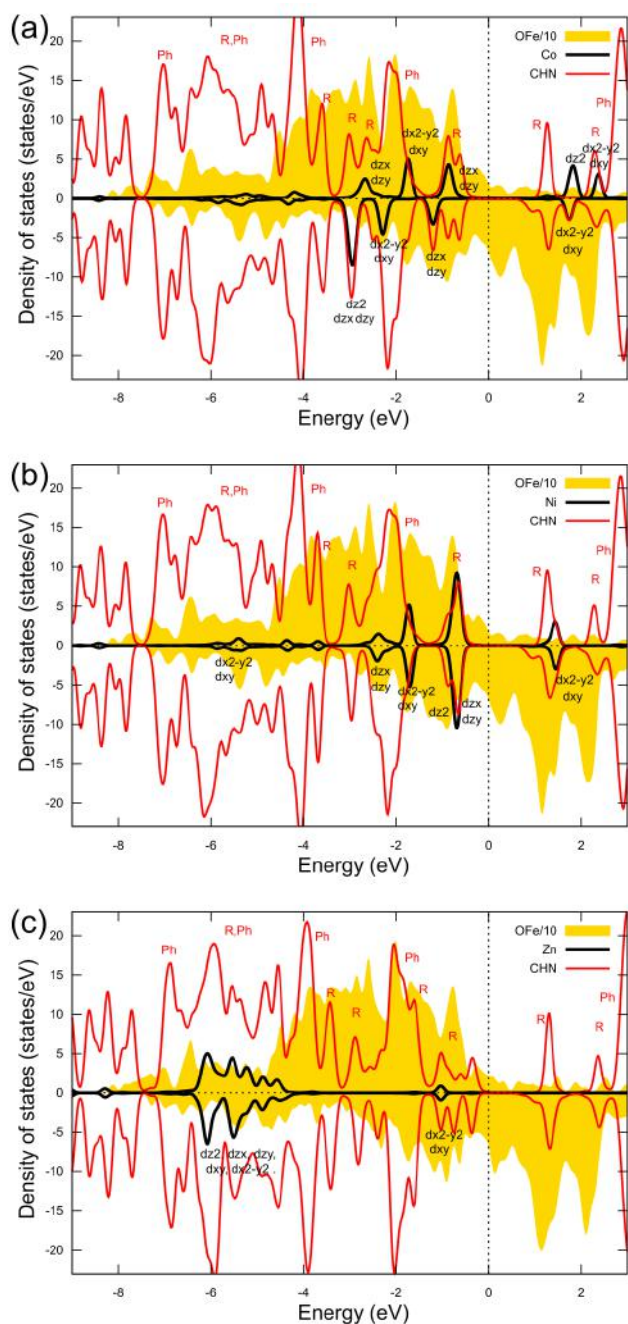
Figure 6: Computed density of states of (a) Co-TPP, (b) Ni-TPP, and (c) Zn-TPP on Fe(001)-($p1 \times 1$)O. The DOS for the spin minority component is shown reversed. The shaded area marks the contribution by the substrate atoms; the black thick line the contribution by the central metal atom and the red thin one by C, H, and N in the molecule. Black labels mark the symmetry of d states (e.g., d_{z^2}) and red labels mark the location of molecular states over the phenyls (Ph) or the tetra-pyrrole ring (R). Data for Co reproduce those published in [29].
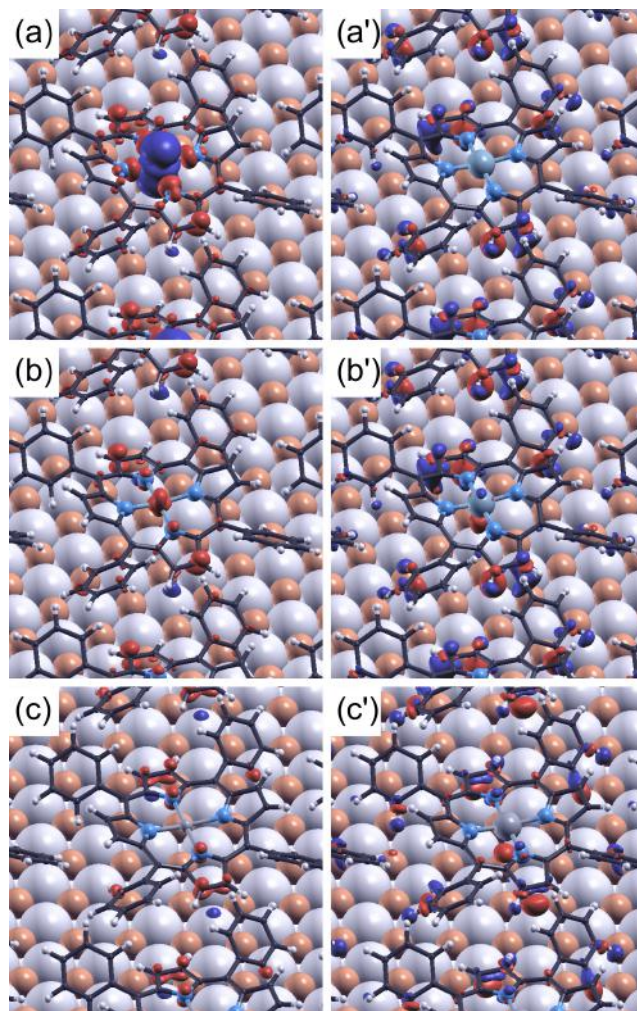
Figure 7: Left panels: Electron spin density for (a) Co-TPP/(5×5)R37°@Fe, (b) Ni-TPP/(5×5)R37°@Fe, and (c) Zn-TPP/(5×5)@O. The chosen isovalue is ±0.005 Å^{-3}. Red/blue surfaces correspond to the spin majority/minority populations. The overwhelming spin density of the free surface is subtracted for image clarity. Right panels: Electron density displacement for (a') Co-TPP, (b') Ni-TPP, and (c') Zn-TPP (all in the same geometries as in the left panels). The chosen isovalue is 0.005 Å^{-3}. Red/blue surfaces in the perspective views correspond to electron accumulation/depletion.

References

[1] B. Kumar, B. Kaushik, N. Y.S., Perspectives and challenges for organic thin film transistors: materials, devices, processes and applications, Nature Comm. 25 (2014) 1–30 (2014). doi:10.1007/s10854-013-1550-2.

[2] A. K. Ray, Organic Materials for Chemical Sensing, Springer International Publishing, 2017 (2017). doi:10.1007/978-3-319-48933-9_52.

[3] N. Seiki, Y. Shoji, T. Kajitani, F. Ishiwari, A. Kosaka, T. Hikima, M. Takata, T. Someya, T. Fukushima, Rational synthesis of organic thin films with exceptional long-range structural integrity, Science 348 (2015) 1122–1126 (2015). doi:10.1126/science.aab1391.

[4] J. M. Gottfried, Surface chemistry of porphyrins and phthalocyanines, Surf. Sci. Rep. 70 (2015) 259–379 (2015). doi:10.1016/j.surfrep.2015.04.001.

[5] F. Buchner, I. Kellner, W. Hieringer, A. Görling, H.-P. Steinrück, H. Marbach, Ordering aspects and intramolecular conformation of tetraphenylporphyrins on Ag(111), Physical Chemistry Chemical Physics 12 (2010) 13082 (2010). doi:10.1039/c004551a.

[6] C. Klingshirn, ZnO: Material, Physics and Applications, ChemPhysChem 8 (2007) 782–803 (2007). doi:10.1002/cphc.200700002.

[7] J. Brede, M. Linares, S. Kuck, J. Schwöbel, A. Scarfato, S.-H. Chang, G. Hoffmann, R. Wiesendanger, R. Lensen, P. H. J. Kouwer, et al., Dynamics of molecular self-ordering in tetraphenyl porphyrin monolayers on metallic substrates, Nanotechnology 20 (2009) 275602 (2009). doi:10.1088/0957-4484/20/27/275602.

[8] L. Scudiero, D. E. Barlow, U. Mazur, K. W. Hipps, Scanning Tunneling Microscopy, Orbital-Mediated Tunneling Spectroscopy, and Ultraviolet Photoelectron Spectroscopy of Metal(II) Tetraphenylporphyrins Deposited from Vapor, Journal of the American Chemical Society 123 (2001) 4073–4080 (2001). doi:10.1021/ja0100726.

[9] J. Xiao, S. Ditze, M. Chen, F. Buchner, M. Stark, M. Drost, H.-P. Steinrück, J. M. Gottfried, H. Marbach, Temperature-Dependent Chemical and Structural Transformations from 2H-tetraphenylporphyrin to Copper(II)-Tetraphenylporphyrin on Cu(111), The Journal of Physical Chemistry C 116 (2012) 12275–12282 (2012). doi:10.1021/jp301757h.

[10] M. Röckert, S. Ditze, M. Stark, J. Xiao, H.-P. Steinrück, H. Marbach, O. Lytken, Abrupt Coverage-Induced Enhancement of the Self-Metalation of Tetraphenylporphyrin with Cu(111), The Journal of Physical Chemistry C 118 (2014) 1661–1667 (2014). doi:10.1021/jp412121b.

[11] S. Fatayer, R. G. A. Veiga, M. J. Prieto, E. Perim, R. Landers, R. H. Miwa, A. de Siervo, Self-assembly of NiTPP on Cu(111): a transition from disordered 1D wires to 2D chiral domains, Physical Chemistry Chemical Physics 17 (2015) 18344–18352 (2015). doi:10.1039/C5CP01288K.

[12] G. Bussetti, A. Calloni, M. Celeri, R. Yivlialin, M. Finazzi, F. Bottegoni, L. Duò, F. Ciccacci, Structure and electronic properties of Zn-tetra-phenyl-porphyrin single- and multi-layers films grown on Fe(001)- p(1 x 1)O, Applied Surface Science 390 (2016) 856–862 (2016). doi:10.1016/j.apsusc.2016.08.137.

[13] S. Rangan, C. Ruggieri, R. Bartynski, J. I. Martínez, F. Flores, J. Ortega, Densely Packed ZnTPPs Monolayer on the Rutile TiO 2 (110)-(1 x 1) Surface: Adsorption Behavior and Energy Level Alignment, The Journal of Physical Chemistry C 120 (2016) 4430–4437 (2016). doi:10.1021/acs.jpcc.5b12736.

[14] G. Lovat, D. Forrer, M. Abadia, M. Dominguez, M. Casarin, C. Rogero, A. Vittadini, L. Floreano, On-Surface Synthesis of a Pure and Long-Range-Ordered Titanium(IV)-Porphyrin Contact Layer on Titanium Dioxide, The Journal of Physical Chemistry C 121 (2017) 13738–13746 (2017). doi:10.1021/acs.jpcc.7b03157.

[15] G. Bussetti, M. Campione, M. Riva, A. Picone, L. Raimondo, L. Ferraro, C. Hogan, M. Palummo, A. Brambilla, M. Finazzi, L. Duò, A. Sassella, F. Ciccacci, Stable Alignment of Tautomers at Room Temperature in Porphyrin 2D Layers, Adv. Funct. Mater. 24 (2014) 958–963 (2014). doi:10.1002/adfm.201301892.

[16] A. Picone, D. Giannotti, A. Brambilla, G. Bussetti, A. Calloni, R. Yivlialin, M. Finazzi, L. Duò, F. Ciccacci, A. Goldoni, et al., Local structure and morphological evolution of Zn-TPP molecules grown on Fe(001)-p(1x1)O studied by STM and NEXAFS, Applied Surface Science 435 (2018) 841–847 (2018). doi:10.1016/j.apsusc.2017.11.128.

[17] S. R. Chubb, W. E. Pickett, First-principles determination of giant adsorption-induced surface relaxation in p(1 x 1) O/Fe(001), Physical Review Letters 58 (12) (1987) 1248–1251 (mar 1987). doi:10.1103/PhysRevLett.58.1248.

[18] F. Donati, P. Sessi, S. Achilli, A. Li Bassi, M. Passoni, C. S. Casari, C. E. Bottani, A. Brambilla, A. Picone, M. Finazzi, L. Duò, M. I. Trioni, F. Ciccacci, Scanning tunneling spectroscopy of the Fe(001) - p(1 x 1)O surface, Physical Review B 79 (19) (2009) 195430 (may 2009). doi:10.1103/PhysRevB.79.195430.

[19] A. Picone, D. Giannotti, M. Riva, A. Calloni, G. Bussetti, G. Berti, L. Duò, F. Ciccacci, M. Finazzi, A. Brambilla, Controlling the Electronic and Structural

Coupling of C_{60} Nano Films on Fe(001) through Oxygen Adsorption at the Interface, ACS Applied Materials & Interfaces 8 (2016) 26418–26424 (2016). doi:10.1021/acsami.6b09641.

[20] G. Bussetti, G. Albani, A. Calloni, M. Sangarashettyhalli Jagadeesh, C. Goletti, L. Duò, F. Ciccacci, Persistence of the Co-tetra-phenyl-porphyrin HOMO-LUMO features when a single organic layer is grown onto Cu(1 1 0)-(2 x 1)O, Applied Surface Science 514 (2020) 145891 (2020). doi:10.1016/j.apsusc.2020.145891.

[21] M. S. Jagadeesh, A. Calloni, A. Brambilla, A. Picone, A. Lodesani, L. Duò, F. Ciccacci, M. Finazzi, G. Bussetti, Room temperature magnetism of ordered porphyrin layers on Fe, Appl. Phys. Lett. 115 (2019) 082404 (2019). doi:10.1063/1.5109750.

[22] N. Ballav, C. Wäckerlin, D. Siewert, P. M. Oppeneer, T. A. Jung, Emergence of on-surface magneto-chemistry, The Journal of Physical Chemistry Letters 4 (2013) 2303–2311 (2013). doi:10.1021/jz400984k.

[23] A. Picone, A. Brambilla, A. Calloni, L. Duò, M. Finazzi, F. Ciccacci, Oxygen-induced effects on the morphology of the Fe(001) surface in out-of-equilibrium conditions, Physical Review B 83 (2011) 235402 (2011). doi:10.1103/PhysRevB.83.235402.

[24] C. Castellarin-Cudia, P. Borghetti, G. Di Santo, M. Fanetti, R. Larciprete, C. Cepek, P. Vilmercati, L. Sangaletti, A. Verdini, A. Cossaro, L. Floreano, A. Morgante, A. Goldoni, Substrate Influence for the Zn-tetraphenyl-porphyrin Adsorption Geometry and the Interface-Induced Electron Transfer, ChemPhysChem 11 (2010) 2248–2255 (2010). doi:10.1002/cphc.201000017.

[25] L. Floreano, A. Cossaro, R. Gotter, A. Verdini, G. Bavdek, F. Evangelista, A. Ruocco, A. Morgante, D. Cvetko, Periodic Arrays of Cu-Phthalocyanine Chains on Au(110), The Journal of Physical Chemistry C 112 (2008) 10794–10802 (2008). doi:10.1021/jp711140e.

[26] T. Thonhauser, S. Zuluaga, C. A. Arter, K. Berland, E. Schröder, P. Hyldgaard, Spin signature of nonlocal correlation binding in metal-organic frameworks, Physical Review Letters 115 (2015) 136402 (2015). doi:10.1103/PhysRevLett.115.136402.

[27] P. Giannozzi, S. Baroni, N. Bonini, M. Calandra, R. Car, C. Cavazzoni, D. Ceresoli, G. L. Chiarotti, M. Cococcioni, I. Dabo, et al., QUANTUM ESPRESSO: a modular and open-source software project for quantum simulations of materials, Journal of Physics: Condensed Matter 21 (2009) 395502 (2009). doi:10.1088/0953-8984/21/39/395502.

[28] P. Giannozzi, O. Andreussi, T. Brumme, O. Bunau, M. B. Nardelli, M. Calandra, R. Car, C. Cavazzoni, D. Ceresoli, M. Cococcioni, et al., Advanced capabilities for materials modelling with QUANTUM ESPRESSO, J. Phys.: Condens. Matter 29 (2017) 465901 (2017). doi:10.1088/1361-648X/aa8f79.

[29] A. Calloni, M. Jagadeesh, G. Bussetti, G. Fratesi, S. Achilli, A. Picone, A. Lodesani, A. Brambilla, C. Goletti, F. Ciccacci, L. Duò, M. Finazzi, A. Goldoni, A. Verdini, L. Floreano, Cobalt atoms drive the anchoring of co-tpp molecules to the oxygen-passivated Fe(001) surface, Applied Surface Science (2019) 144213 (2019). doi:https://doi.org/10.1016/j.apsusc.2019.144213.

[30] A. Picone, G. Fratesi, A. Brambilla, P. Sessi, F. Donati, S. Achilli, L. Maini, M. I. Trioni, C. S. Casari, M. Passoni, et al., Atomic corrugation in scanning tunneling microscopy images of the Fe(001)-p(1x1)O surface, Physical Review B 81 (2010) 115450 (2010). doi:10.1103/PhysRevB.81.115450.

[31] A. Picone, M. Riva, G. Fratesi, A. Brambilla, G. Bussetti, M. Finazzi, L. Duò, F. Ciccacci, Enhanced atom mobility on the surface of a metastable film, Physical Review Letters 113 (2014) 046102 (2014). doi:10.1103/PhysRevLett.113.046102.

[32] M. Riva, A. Picone, D. Giannotti, A. Brambilla, G. Fratesi, G. Bussetti, L. Duò, F. Ciccacci, M. Finazzi, Mesoscopic organization of cobalt thin films on clean and oxygen-saturated Fe(001) surfaces, Phys. Rev. B 92 (2015) 115434 (2015). doi:10.1103/PhysRevB.92.115434.

[33] A. Dal Corso, Pseudopotentials periodic table: From H to Pu, Computational Materials Science 95 (2014) 337–350 (2014). doi:10.1016/j.commatsci.2014.07.043.

[34] H. J. Monkhorst, J. D. Pack, Special points for brillouin-zone integrations, Physical Review B 13 (1976) 5188–5192 (1976). doi:10.1103/PhysRevB.13.5188.

[35] A. M. Ritzmann, M. Pavone, A. B. Muñoz-García, J. A. Keith, E. A. Carter, Ab initio DFT+U analysis of oxygen transport in LaCoO3: the effect of Co3+ magnetic states, J. Mater. Chem. A 2 (2014) 8060–8074 (2014). doi:10.1039/C4TA00801D.

[36] S.-J. Hu, S.-S. Yan, M.-W. Zhao, L.-M. Mei, First-principles LDA + U calculations of the co-doped ZnO magnetic semiconductor, Phys. Rev. B 73 (2006) 245205 (2006). doi:10.1103/PhysRevB.73.245205.

[37] K. Leung, S. B. Rempe, P. A. Schultz, E. M. Sproviero, V. S. Batista, M. E. Chandross, C. J. Medforth, Density Functional Theory and DFT + U Study of Transition

Metal Porphines Adsorbed on Au(111) Surfaces and Effects of Applied Electric Fields, J. Am. Chem. Soc. 128 (2006) 3659–3668 (2006). `doi:10.1021/ja056630o`.

[38] M.-S. Liao, S. Scheiner, Electronic structure and bonding in metal porphyrins, metal=Fe, Co, Ni, Cu, Zn, The Journal of Chemical Physics 117 (2002) 205–219 (2002). `doi:10.1063/1.1480872`.

[39] N. Schmidt, R. Fink, W. Hieringer, Assignment of near-edge x-ray absorption fine structure spectra of metalloporphyrins by means of time-dependent density-functional calculations, The Journal of Chemical Physics 133 (2010) 054703 (2010). `doi:10.1063/1.3435349`.

[40] G. Zamborlini, M. Jugovac, A. Cossaro, A. Verdini, L. Floreano, D. Lüftner, P. Puschnig, V. Feyer, C. M. Schneider, On-surface nickel porphyrin mimics the reactive center of an enzyme cofactor, Chemical Communications 54 (2018) 13423–13426 (2018). `doi:10.1039/C8CC06739B`.

[41] W. Auwärter, K. Seufert, F. Klappenberger, J. Reichert, A. Weber-Bargioni, A. Verdini, D. Cvetko, M. Dell'Angela, L. Floreano, A. Cossaro, et al., Site-specific electronic and geometric interface structure of Co-tetraphenyl-porphyrin layers on Ag(111), Physical Review B 81 (2010) 245403 (2010). `doi:10.1103/PhysRevB.81.245403`.

[42] D. Wechsler, M. Franke, Q. Tariq, L. Zhang, T.-L. Lee, P. K. Thakur, N. Tsud, S. Bercha, K. C. Prince, H.-P. Steinrück, et al., Adsorption Structure of Cobalt Tetraphenylporphyrin on Ag(100), The Journal of Physical Chemistry C 121 (2017) 5667–5674 (2017). `doi:10.1021/acs.jpcc.7b00518`.

[43] C. Ruggieri, S. Rangan, R. A. Bartynski, E. Galoppini, Zinc(II) Tetraphenylporphyrin on Ag(100) and Ag(111): Multilayer Desorption and Dehydrogenation, The Journal of Physical Chemistry C 120 (2016) 7575–7585 (2016). `doi:10.1021/acs.jpcc.6b00159`.

[44] G. Zamborlini, D. Lüftner, Z. Feng, B. Kollmann, P. Puschnig, C. Dri, M. Panighel, G. Di Santo, A. Goldoni, G. Comelli, et al., Multi-orbital charge transfer at highly oriented organic/metal interfaces, Nature Communications 8 (2017) 335 (2017). `doi:10.1038/s41467-017-00402-0`.

[45] P.-O. Löwdin, On the non-orthogonality problem connected with the use of atomic wave functions in the theory of molecules and crystals, The Journal of Chemical Physics 18 (1950) 365 (1950). `doi:10.1063/1.1747632`.

[46] A. Brambilla, A. Picone, D. Giannotti, A. Calloni, G. Berti, G. Bussetti, S. Achilli, G. Fratesi, M. I. Trioni, G. Vinai, P. Torelli, G. Panaccione, L. Duò, M. Finazzi, F. Ciccacci, Enhanced magnetic hybridization of a spinterface through insertion of a two-dimensional magnetic oxide layer, Nano Lett. 17 (2017) 7440 (2017). `doi:10.1021/acs.nanolett.7b03314`.